

# STAFF SUMMARY SHEET

	TO	ACTION	SIGNATURE (Surname), GRADE AND DATE		TO	ACTION	SIGNATURE (Surname), GRADE AND DATE
1	DFAN	sig	<i>Robert Decker, Col</i> 12 Mar 2012	6			
2	DFER	approve	<i>Brent A. Parker Col</i> 12 Mar 2012	7			
3	DFAN	action		8			
4				9			
5				10			
SURNAME OF ACTION OFFICER AND GRADE			SYMBOL	PHONE		TYPIST'S INITIALS	SUSPENSE DATE
C1C Luke			CS-39	333-0669		cgl	20120315
SUBJECT Clearance for Material for Public Release							DATE 20120309
USAFA-DF-PA-102							

## SUMMARY

1. PURPOSE. To provide security and policy review on the document at Tab 1 prior to release to the public.

## 2. BACKGROUND.

Authors: Robert K Decker, C1C Christopher Luke, C1C Stephanie Sexton,

Title: Measuring Skin Friction Drag over a Flat Plate Using Thin Oil Film Interferometry

Circle one: Abstract      Tech Report      Journal Article      Speech       Paper      Presentation      Poster  
 Thesis/Dissertation      Book      Other: \_\_\_\_\_

Check all that apply (For Communications Purposes):

Description: Skin friction drag is a difficult aerodynamic property to measure on a wind tunnel model and hard to predict using computational fluid dynamics. One solution which may help improve and/or solve some of these issues is an experimental method called Thin Oil Film Interferometry (TOFI). After several semesters of research, the accuracy of this method has been reduced to within 40-60% of theoretical values. By assuming 1-D, incompressible, turbulent flow over a flat plate, the skin friction can be calculated using relatively simple equations. TOFI measures the skin friction on a flat plate by relating the phase shift of light captured in an interference pattern to the changing height in oil as it is pushed along the flat plate in a wind tunnel. The skin friction coefficient can be determined from the oil height profile. Current research serves to make qualitative improvements to ensure that the assumptions made for the flat plate are as close as possible to ideal. The accuracy of the skin friction coefficient can be confirmed by ensuring that these variables hold true in the experiment. These qualitative improvements have shown to greatly improve the accuracy of the method by reducing the percent error down to within 7-11%. Future research hopes to apply this method to more complex geometries.

Release Information: To be presented at the AIAA Student Paper Competition, Boulder CO, April 4-6, 2012

Recommended Distribution Statement: Distribution A: approved for public release, distribution unlimited

## 3. DISCUSSION.

4. RECOMMENDATION. Sign coord block above indicating document is suitable for public release. Suitability is based solely on the document being unclassified, not jeopardizing DoD interests, and accurately portraying official policy.

*Thomas E. McLaughlin*  
 Thomas E. McLaughlin, Ph.D.  
 Director, Aeronautics Research Center

# Measuring Skin Friction Drag over a Flat Plate Using Thin Oil Film Interferometry

Chris Luke<sup>1</sup> and Stephanie Sexton<sup>2</sup>

*Department of Aeronautics, Colorado Springs, CO, 80840*

Robert Decker<sup>3</sup>

*Department of Aeronautics, Colorado Springs, CO, 80840*

Skin friction drag is a difficult aerodynamic property to measure on a wind tunnel model and hard to predict using computational fluid dynamics. One solution which may help improve and/or solve some of these issues is an experimental method called Thin Oil Film Interferometry (TOFI). After several semesters of research, the accuracy of this method has been reduced to within 40-60% of theoretical values. By assuming 1-D, incompressible, turbulent flow over a flat plate, the skin friction can be calculated using relatively simple equations. TOFI measures the skin friction on a flat plate by relating the phase shift of light captured in an interference pattern to the changing height in oil as it is pushed along the flat plate in a wind tunnel. The skin friction coefficient can be determined from the oil height profile. Current research serves to make qualitative improvements to ensure that the assumptions made for the flat plate are as close as possible to ideal. The accuracy of the skin friction coefficient can be confirmed by ensuring that these variables hold true in the experiment. These qualitative improvements have shown to greatly improve the accuracy of the method by reducing the percent error down to within 7-11%. Future research hopes to apply this method to more complex geometries.

## Nomenclature

$C_f$	=	Skin friction coefficient
$h$	=	oil height
$n_a$	=	index of refraction of air
$n_f$	=	index of refraction of oil
$cSt$	=	centistoke(s)
$q$	=	dynamic pressure
$Re_x$	=	Reynolds Number
$t$	=	time
$U_\infty$	=	freestream velocity
$x$	=	distance from leading edge
$\tau_w$	=	shear stress at wall
$\theta_i$	=	incidence angle of light
$\rho$	=	density
$\mu$	=	dynamic viscosity
$\nu$	=	kinematic viscosity
$\lambda$	=	light wavelength
$\phi$	=	phase shift

<sup>1</sup> Cadet Second Class, PO Box 2855, Department of Aeronautics

<sup>2</sup> Cadet Second Class, PO Box 4586, Department of Aeronautics

<sup>3</sup> Research Engineer, Department of Aeronautics, Member AIAA

## I. Introduction

Currently, aerodynamicists do not have a closed form solution to calculate skin friction drag. The Thin Oil Film Interferometry (TOFI) method for experimentally measuring skin friction drag over a flat plate can serve as a possible baseline for skin friction calculations on larger, more complicated surfaces. If this method can be proven accurate, corrections can be applied to computational fluid dynamics (CFD) models of predicting skin friction. These improvements will allow CFD approximations to be more accurate in predicting real world issues with flight systems. With a reliable method of measuring skin friction drag, aerodynamicists will be able to improve the overall efficiency of aircraft.

TOFI uses the changing height of an oil film to calculate the skin friction. This is done by using several equations that take into account the phase shift of light as it passes through the oil. TOFI captures this phase shift in an interference pattern created by light reflected off the surface of a flat plate and captured by a camera. As seen in Figure 1, a specific wavelength ( $\lambda$ ) light source is set up at a certain incidence angle  $\theta_i$  to the flat plate and a camera is mounted opposite of the light source. This wavelength of light is shone onto the oil and flat plate as flow passes over. Some light is reflected off of the oil and some refracts through the oil. The refracted light continues to travel through the oil and reflects off of the surface of the flat plate. This difference in distance traveled by the light creates a phase shift which is captured through the camera, as an interference pattern that shows up as light and dark bands on the surface as seen in the top of Figure 1.

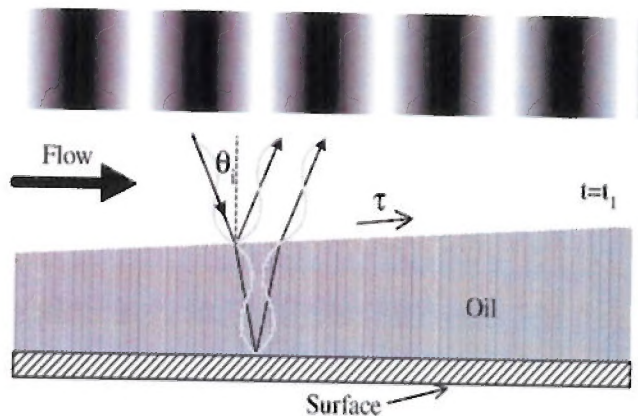


**Figure 1. Interferometry Diagram of oil being pushed along a flat surface as flow passes over and the interference pattern created by the phase change of the light wave<sup>1</sup>**

After obtaining the interference pattern, the distance between bands can be related directly to the phase shift of the light. With this phase shift, Equation 1 can be used to calculate the height of the oil at that point.

$$h = \frac{\lambda\phi}{4\pi} \left( \frac{1}{\sqrt{n_f^2 - n_a^2 \sin\theta_i}} \right) \quad (1)^1$$

Where  $\phi$  is the phase shift of the light wave,  $n_f$  is the index of refraction of the oil,  $n_a$  is the index of refraction of the air,  $\theta_i$  is the incidence angle of the incoming light wave, and  $\lambda$  is the wavelength of the light. Using the height of the oil, the skin friction coefficient can be found using Equation 2.

$$C_f = \frac{\mu \Delta x}{q \Delta h t} \quad (2)^2$$

Where  $\mu$  is the dynamic viscosity of the oil,  $q$  is the dynamic pressure during the run,  $\Delta h$  is the change in height of the oil from one distance to another, and  $t$  is the time elapsed. It is important to note that the  $\Delta x$  in Equation 3 is the  $x$  distance where  $\Delta h$  was measured. Theoretically, the approximation of the skin friction coefficient for a turbulent boundary layer on a flat plate can easily be calculated using Reynolds number, see Equation 3.

$$C_f \approx \frac{0.455}{\ln(0.06Re_x)^2} \quad (3)^2$$

The experimentally calculated value of the skin friction can be compared to the theoretically obtained value to comprehend how accurately the TOFI method measures skin friction.

Skin friction is a very difficult variable to measure in real world flight test scenarios. Additionally, CFD cannot produce accurate predictions for skin friction. If aerodynamicists can find a way to accurately predict the skin friction drag on an aircraft, the accuracy of CFD models can be improved thus giving a better prediction of flight test data. Being able to predict skin friction drag is important because aerodynamicists will be able to find ways to

reduce total drag, indirectly increasing the overall fuel efficiency of an aircraft. The overall objective of this experiment is to improve the accuracy of previous semesters' research and more specifically, make qualitative improvements to be confident the experiment has simple, 1-D, incompressible, turbulent flow over the flat plate. By ensuring that the each assumption is valid, the accuracy of the method can be determined. After the method is proven to be accurate for a simple flat plate, the method can then be applied to more complex aircraft geometries.

## II. Set-up and Procedure

The experiment was conducted in the United States Air Force Academy's Aeronautics Laboratory in the cascade wind tunnel. This tunnel is closed loop with flow cooling, a maximum Mach of 0.2, and a 6.75 square foot Plexiglas test section. The test section is ideal for interferometry because accurate images can be taken of the oil on the plate through the clear Plexiglas material. The plate is composed of black painted Plexiglas with a rounded leading edge and an inlaid piece of polished stainless steel. There are "winglets" or side fences attached to each edge of the plate to prevent any 2-D flow. Along the edge of the inlaid stainless steel, three pressure ports have been added to measure the static pressure to determine the pressure gradient along the plate. Additionally, in the inlaid stainless steel there are two thermocouples that measure the temperature at the front edge and the back edge. These temperatures are used to determine the viscosity of the oil. See Figures 2 through 4 for a visual representation of the test setup.

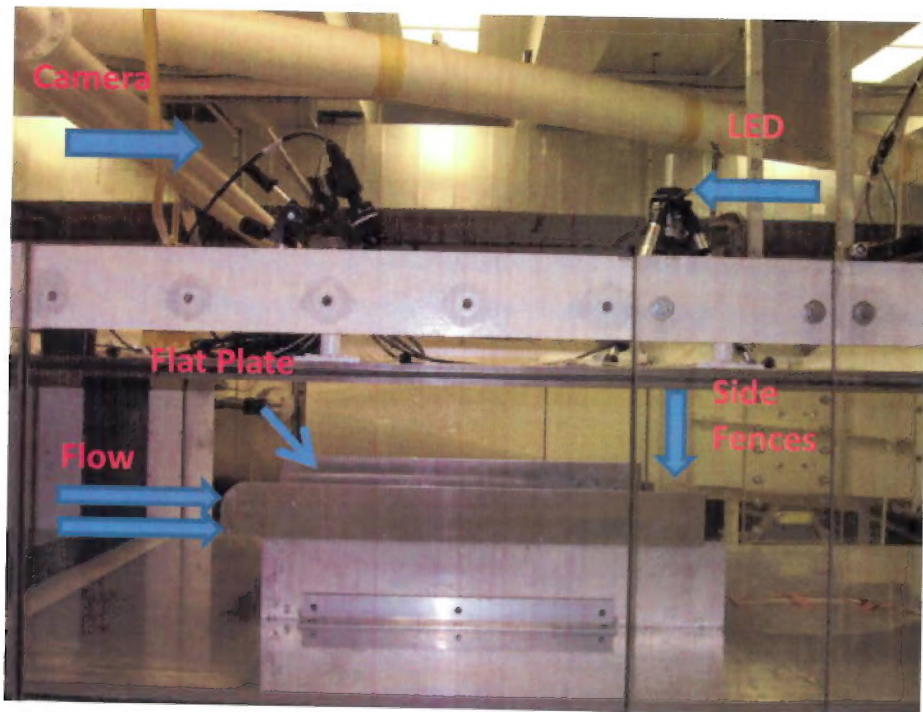


Figure 2. Side View of Equipment Setup



Figure 3. Oblique View of Setup

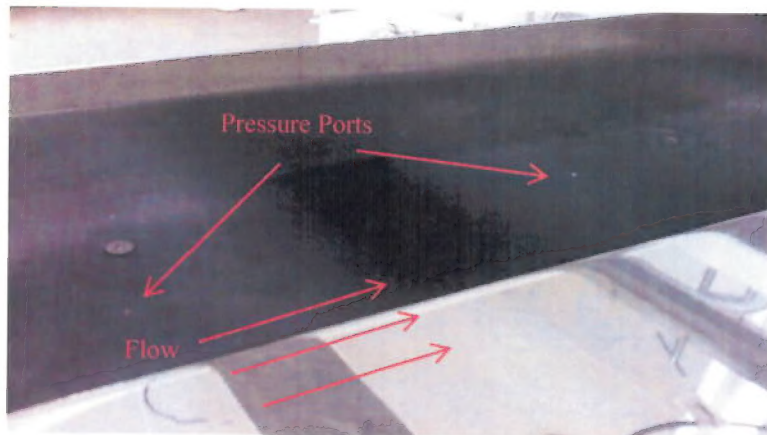


Figure 4. Close Up Showing Proximity of Pressure Ports to Polished Plate

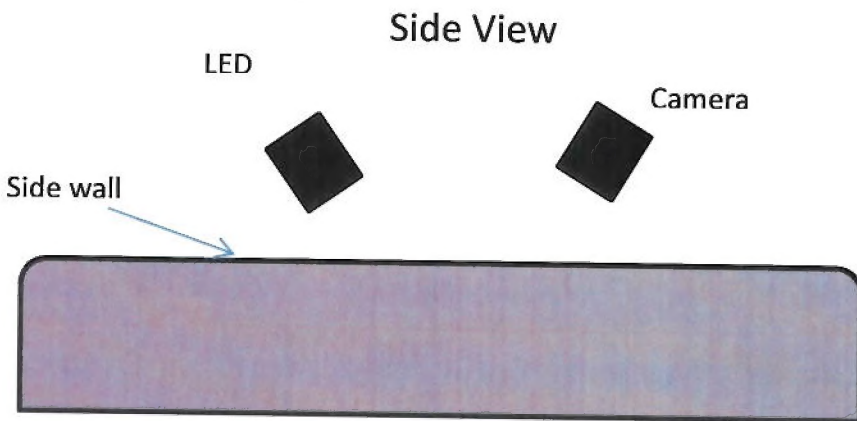
As seen in Figure 2, the camera and LED light are situated at equal offset angles from the plate. Table 1 lists all the equipment used for the test.

Table 1. Equipment List

Item	Manufacturer	Model #	Range	Uncertainty	Calibration Date
Camera	Cohu	7700	1004x1004 pixels	N/A	N/A
Camera Card	National Instruments	PCI-1428	N/A	N/A	N/A
LED Light	Edmund Optics	NT 64-928	470 nm	N/A	N/A
Optical Bandpass Filter	Edmund Optics	NT 65-687	400-490 nm	N/A	N/A
Thermocouple wire	Omega Eng	EXPP-T-20-TWSM	N/A	1 deg C	N/A

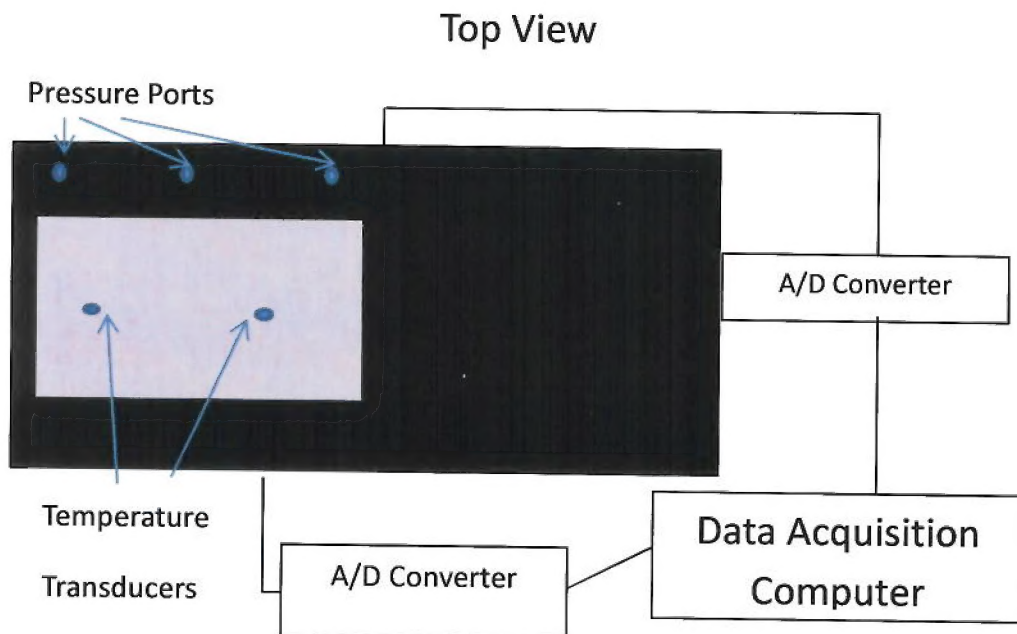
Silicon Oils	Dow Corning	510 Fluid	100 cSt	1.5 cSt	27-Aug-10
Pressure Transducer A/D Converter box	National Instruments	NI 9215	$\pm 40$ Torr	N/A	N/A
Pressure Transducer (differential)	MKS Instruments	220-D-26482	40 Torr	1% of Full Scale	10-Jan-12
Thermocouple A/D converter Box	National Instruments	NI9211	$\pm 80$ mV	N/A	N/A
Pressure Transducer (differential)	Scaniavaive Corp.	DSA3217	$\pm 1$ Psi	1% of Full Scale	7-Jul-11

Figure 5 shows a side view of the plate in the test section and a view of the locations of equipment relative to the plate, as well as shows a more detailed depiction of the angle between the plate, LED, and the camera.



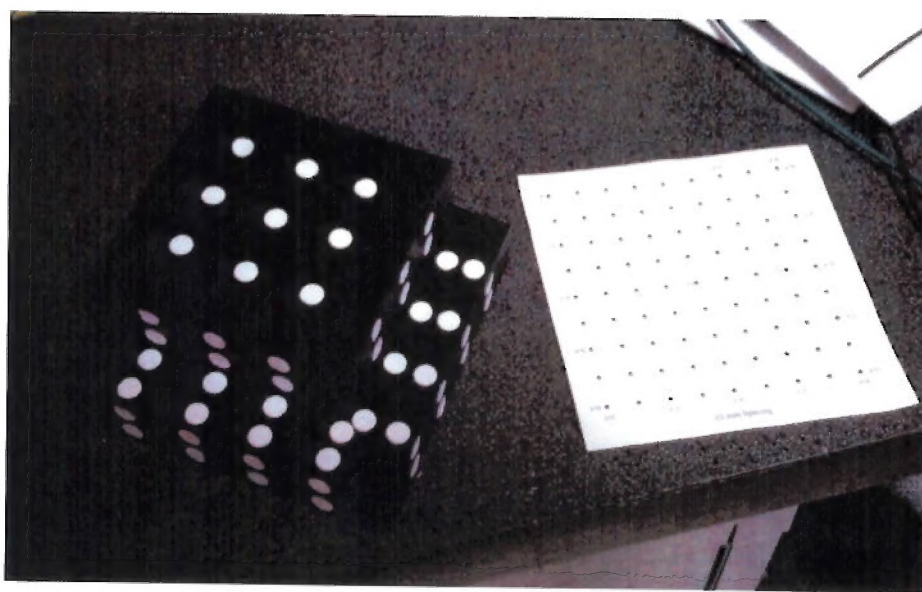
**Figure 5. Side View of Plate with Fence**

Figure 6 is a bird's eye view looking down onto the top of the test section and the location of how all of the equipment is connected to the plate and computer. Once the full setup has been completed and the tunnel has been secured, the test can commence.



**Figure 6. Top View Schematic**

The experiment begins by first taking two calibration photos for purposes of data analysis. The first calibration photo is taken of the 3-D calibration block which is seen on the left side of Figure 7.



**Figure 7. Calibration Equipment<sup>3</sup>**

This block enables the analysis software to understand the characteristics of the optical system used to capture the images. The second calibration image utilizes the white sheet seen on the right side of Figure 7. This sheet has black

dots at spacing intervals of 10mm. The calibration image of this piece gives the software a distance reference which is then applied to the experimental images to determine the spacing between the light and the dark bands. The location of the calibration piece is noted by laying a ruler next to it in the image. This ruler has its zero point at the leading edge of the plate and allows the calibration image to also note the distance back from the leading edge where the measurements are being taken. After the calibration is complete, the flat reflective plate is cleaned with a standard household cleaning agent to ensure that there is no left over residue from a previous run. Then, a thin line of oil is applied to the reflective plate perpendicular to the flow using a Popsicle stick, seen in Figure 8. The Popsicle stick absorbs some of the oil and as it is placed on the plate, the oil leeches out into the straight line seen in Figure 9.



**Figure 8. Oil Application**

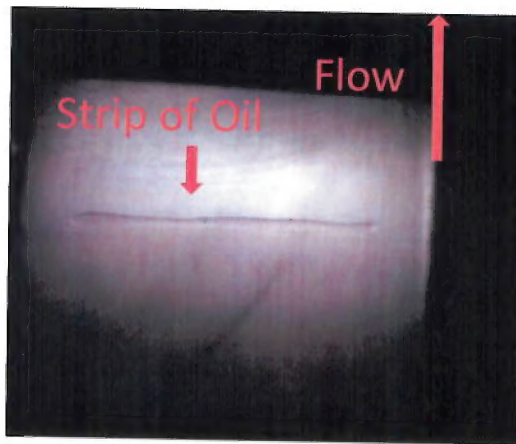


**Figure 9. Oil Setup**

The exact location of the oil does not need to be recorded because the second calibration image is taken with note to the distance from the leading edge. Once the oil has been applied, the tunnel is secured and the data acquisition software is started. The tunnel motor is immediately brought up to 45 Hz to avoid startup transients as much as

possible. Once the motor has been brought to speed, the fan blades are pitched to the #5 setting on the dial to achieve a Mach number of 0.1. The tunnel is run until the oil has reached a constant wedge shape and the fringe patterns in the oil can be seen. After steady state has been reached, the data acquisition program is stopped, the motor is decelerated to zero, the fan blades are pitched to zero, and the tunnel is turned off. At this point, all required data for the analysis of skin friction has been collected for the experiment. The tunnel is then opened up and the oil is cleaned off of the flat plate.

The data collected in each run consists of images of the interference pattern, dynamic pressure readings, static pressure readings, temperature readings, and the time the tunnel was run. These runs can be seen in the original test matrix in Table 2, which contains the relative location of the oil from the leading edge of the plate and the type of setup used. Runs 11 and 12 were replacement runs for runs 10 and 5, respectively. The test runs shown in the second test matrix in Table 3 were completed to overcome confusion in the placement of the oil on the plate and bad focus of the camera.

**Table 2. Test Matrix of First Six Runs**

Run	Location (m)	Oil	Setup
5	Back	100 cSt	No Sandpaper
6	Middle	100 cSt	No Sandpaper
7	Front	100 cSt	No Sandpaper
8	Front	100 cSt	Solid Sandpaper Strip
9	Middle	100 cSt	Solid Sandpaper Strip
10	Back	100 cSt	Solid Sandpaper Strip

**Table 3. Re-Run Test Matrix**

Run	Location (m)	Oil	Setup
11	Back	100 cSt	Solid Sandpaper Strip
12	Back	100 cSt	No Sandpaper

The images are the main data used in analysis, the pressure data is used to determine wind tunnel speed, and temperature data is used to determine the viscosity of the oil on the reflective plate. Once all the data has been collected with the Labview program, the analysis is conducted in MATLAB. Each calibration image is analyzed by the MATLAB software program to determine an axis system. Once an axis system is established, the software can

determine where to analyze each oil film image to find the skin friction coefficient data. The user determines where the analysis should be done on each image and sets up analysis lines that are parallel to the flow as seen in Figure 10.

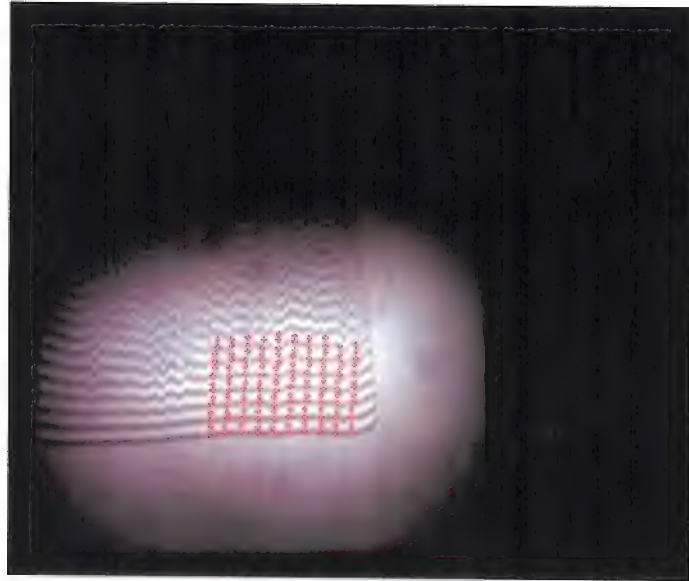


**Figure 10. Analysis Lines Where the Fourier Transform Will Be Calculated (Flow Goes From Bottom to Top)**

Each of the analysis lines is then put through a Fourier Transform to find the dominate frequency that represents the change between the light and dark bands. This information is used to filter out the noise to allow the software to find the distance between each band. After the distances are determined, the Equations 1 and 2 are used to calculate the skin friction coefficient for multiple spots along the analysis line. After each analysis line has been completed, the skin friction coefficient values are grouped by the distance from the leading and output into a histogram like plot. With these plots, a comparison of the theoretical values can be used to determine the accuracy of the method.

### **III. Results and Discussion**

A total of 6 test runs were completed in order to meet the objectives of this semester's experiment. To ensure the 1-D assumption was met, side fences were added to the flat plate. These side fences seem to have stopped all of the cross plate flow thus allowing the experiment to meet the 1-D assumption. Also the pressure ports that were added to determine pressure gradient showed a 0.001 psi difference in static pressure between the front of the plate and the back of the plate. Since the bias error of the pressure transducer device is zero from the calibration and

the uncertainty is orders of magnitude smaller than one psi, the assumption can be made that there is little to no pressure gradient along the plate. This also meets the assumption of the theoretical equations. In this experiment, runs 1-4 were test runs to both get the equipment set up and allow the researchers to get comfortable with the test procedures and setup. These runs were also used to help reduce the amount of dust running through the tunnel, which may have collected in the oil and interfered with the patterns picked up by the camera. This was done by inserting filters to help catch some of the dust as the tunnel ran. For runs 5, 6, and 7, no sand paper was added to the leading edge of the flat plate. For runs 8, 9, and 10, sand paper was added to ensure that turbulent flow was present over the flat plate in order to match the theoretical approximations for skin friction to the experimental measurements. Runs 5 through 7 were conducted at different locations along the flat plate approximately, 0.3, 0.4 and 0.5 feet back from the leading edge. Similarly, runs 8 through 10 were also conducted at different locations along the plate in the front, middle, and back.

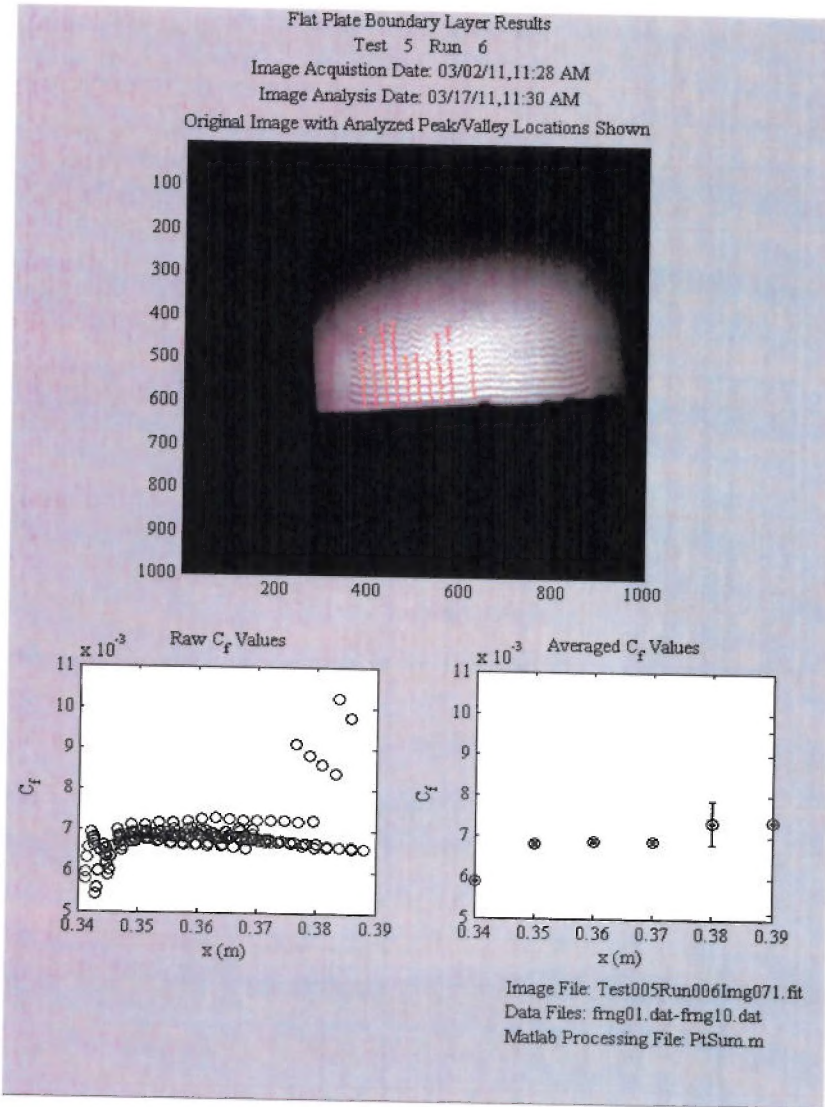


**Figure 11. Run 6 Analysis Results from Run 6 (Flow From Bottom to Top)**

The results of each run were summarized into a figure similar to the one seen in Figure 11, which shows the individual results of run 6. The picture seen at the top of Figure 11 is an image from the final run with the analysis lines used by MATLAB to compute the skin friction along the plate marked in red. The data points are only collected along these lines. The graph in the lower left corner of the picture is the raw data with  $x$ , the distance along the flat plate on the  $x$  axis, and the  $C_f$  value along the  $y$  axis. The  $x$  distance is used on this graph instead of Reynolds Number because the only significant variance in Reynolds Number is the distance along the plate. This graph shows that the  $C_f$  values for run 6 are around 0.006 throughout the short change in  $x$  distance along the photo. This graph is useful because verifies the results obtained are consistent and reasonably well clustered for each run. The other graph combines all the data points between the previous average point and the average point for that bin.

The data is binned by averaging all the values between two x values and locating them at the top x value of the range. The bars shown are standard error bars, these bars are calculated using Equation 4.

$$\frac{C_{f_{std}}}{\sqrt{N}} \quad (4)$$

Where  $C_{f_{std}}$  is the standard deviation in the  $C_f$  values and N is the number of values that are within that bin. Thus with a larger amount of samples in a given bin, the smaller the standard error will be regardless of a large standard deviation.

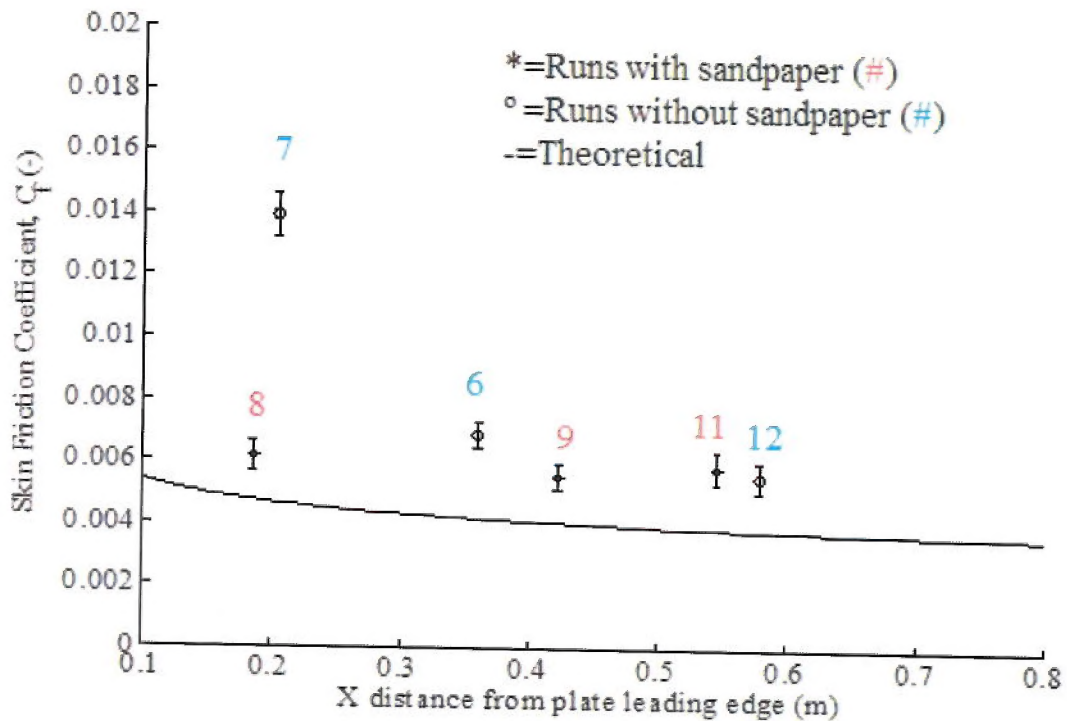


**Figure 12. Summary Plot of All Six Runs**

The plot in Figure 12 shows each run with the sandpaper and non-sandpaper cases clearly separated. The solid line is the theoretical value of skin friction. As seen in the figure, the runs with the sandpaper are closer to the theoretical value, while the runs without the sandpaper are somewhat scattered. Therefore, the conclusion can be drawn that adding a solid strip of sandpaper to the leading edge of the flat plate ensures that the turbulent flow assumption is valid for this experiment.

Overall the results came much closer to theoretical values. For each run a percent error was calculated from the theoretical value which was found using Equation 3 using the actual dynamic pressure of each run. The results can all be seen in Table 5.

**Table 5. Final Results for All Runs**

Run	Location	Conditions	Theoretical $C_f$	Actual $C_f$	% Error
12	0.585	No Sandpaper (Back)	0.00524013	0.005451	4%
6	0.365	No Sandpaper (Middle)	0.00583763	0.00684	17%
7	0.21	No Sandpaper (Front)	0.00657369	0.012928	97%
8	0.195	Sandpaper (Front)	0.00677952	0.00605	11%
9	0.425	Sandpaper (Middle)	0.00559393	0.005509	2%
11	0.546	Sandpaper (Back)	0.00537115	0.0058	8%

The average percent error for the runs with a solid strip of sandpaper on the leading edge was 7% while the average percent error for the runs without the sandpaper was 39%. As seen in Table 5 as well as in Figure 12, run 7 was an outlier to the normal data. The results for run 7 were bad data because the camera was unable to capture a clear image of the interference pattern. The percent error of the runs without the sandpaper not including run 7 was 11% error. These errors were drastically reduced from previous experiments. This shows that the addition of the side fences did in fact allow the experimental conditions to match the conditions specified in the theoretical equation. Another factor that may have reduced the error was the slow Mach number which eliminates some of

the transient start up time of the wind tunnel. Overall the results of this experiment show great progress towards a usable method to find skin friction.

#### **IV. Conclusion**

Results from this experiment support the fact that the strip of sandpaper and side winglets do in fact produce the 1-D, turbulent flow that is assumed in the theoretical calculations. This confirmation leads one to believe that the results from the experiment should be very close to the theoretical values. Because the results showed slightly higher  $C_f$  values compared to theoretical values, there are some other issues with the experiment. One of these issues could be the definition of the front of the plate. Also there could be other factors within the turbulent boundary layer close to the flat plate that are not assumed within the theoretical equations. In the future, more tests should be done on more complex geometries. Since most bodies are not flat plates a method to find skin friction must be found for complex 3-D geometries. Another piece of future work that could be done is the re-arrangement of the test set-up in order to take the interferometry images through the side panel of the wind tunnel. This would eliminate some issues encountered when trying to adjust the camera and LED light source.

#### **VI. Acknowledgments**

The Air Force Office of Scientific Research is funding this project. Thank you to the Lab Technician SSgt Washburn for his technical expertise. Also thank you to Mr. Falkenstine for fabricating our plates.

#### **VII. References**

<sup>1</sup>J. W. Naughton, M. Sheplak, Modern developments in shear stress measurement, *Progress in Aerospace Sciences*, August/October 2002, pp. 515-570

<sup>2</sup>White, F. "Viscous Fluid Flow," 1974, pp. 429-432.

<sup>3</sup>Miller, N., Nelson, T. and Decker, R., "Measuring Skin friction using Thin Oil Interferometry on a Flat Plate," Fall 2010, pp. 1-17.